The Class of Simple Cube-Curves Whose MLPs Cannot Have Vertices at Grid Points

Fajie Li and Reinhard Klette

CITR, University of Auckland, Tamaki Campus,
Building 731, Auckland, New Zealand

Abstract. We consider simple cube-curves in the orthogonal 3D grid of cells. The union of all cells contained in such a curve (also called the tube of this curve) is a polyhedrally bounded set. The curve's length is defined to be that of the minimum-length polygonal curve (MLP) fully contained and complete in the tube of the curve. So far only one general algorithm called rubber-band algorithm was known for the approximative calculation of such a MLP. There is an open problem which is related to the design of algorithms for calculation a 3D MLP of a cube-curve: Is there a simple cube-curve such that none of the vertices of its 3D MLP is a grid vertex? This paper constructs an example of such a simple cube-curve. We also characterize this class of cube-curves.

1 Introduction

The analysis of cube-curves is related to 3D image data analysis. A cube-curve is, for example, the result of a digitization process which maps a curve-like object into a union S of face-connected closed cubes. The length of a simple cube-curve in 3D Euclidean space is based on the calculation of the minimal length polygonal curve (MLP) in a polyhedrally bounded compact set [3, 4].

The computation of the length of a simple cube-curve in 3D Euclidean space was a subject in [5]. But the method may fail for specific curves. [1] presents an algorithm (rubber-band algorithm) for computing the approximating MLP in S with measured time complexity in $O(n)$, where n is the number of grid cubes of the given cube-curve.

The difficulty of the computation of the MLP in 3D may be illustrated by the fact that the Euclidean shortest path problem (i.e., find a shortest obstacle-avoiding path from source point to target point, for a given finite collection of polyhedral obstacles in 3D space and a given source and a target point) is known to be NP-complete [7]. However, there are some algorithms solving the approximate Euclidean shortest path problem in 3D with polynomial-time, see [8]. The Rubber-band algorithm is not yet proved to be always convergent to the correct 3D-MLP.

Recently, [6] developed of an algorithm for calculation of the correct MLP (with proof) for a special class cube-curves. The main idea is to discompose the cube-curve into some arcs by finding some "end angles" (see Definition 4 below).

E. Andres et al. (Eds.): DGCI 2005, LNCS 3429, pp. 183–194, 2005.

There is an open problem (see [2–page 406]) which is related to designing algorithms for the calculation of the 3D MLP of a cube-curve: It there a simple cube-curve such that none of the vertices of its 3D MLP is a grid vertex? This paper constructs an example of such a simple cube-curve, and generalizes this by characterizing the class of all of those cube-curves. Furthermore it is true that these cube-curves do not have any end angle; and this means that we cannot use the MLP algorithm proposed in [6] which is provable correct. This is the basic importance of the given result: we show the existence of cube-curves which require further algorithmic studies.

Following [1], a grid point $(i, j, k) \in \mathbb{Z}^3$ is assumed to be the center point of a *grid cube* with *faces* parallel to the coordinate planes, with *edges* of length 1, and *vertices* as its corners. *Cells* are either cubes, faces, edges, or vertices. The intersection of two cells is either empty or a joint *side* of both cells. A *cube-curve* is an alternating sequence $g = (f_0, c_0, f_1, c_1, \ldots, f_n, c_n)$ of faces f_i and cubes c_i, for $0 \leq i \leq n$, such that faces f_i and f_{i+1} are sides of cube c_i, for $0 \leq i \leq n$ and $f_{n+1} = f_0$. It is *simple* iff $n \geq 4$ and for any two cubes $c_i, c_k \in g$ with $|i - k| \geq 2$ (mod $n + 1$), if $c_i \bigcap c_k \neq \phi$ then either $|i - k| = 2$ (mod $n + 1$) and $c_i \bigcap c_k$ is an edge, or $|i - k| \geq 3$ (mod $n + 1$) and $c_i \bigcap c_k$ is a vertex.

A *tube* $\mathbf{g}$ is the union of all cubes contained in a cube-curve g. A tube is a compact set in $\mathbb{R}^3$, its frontier defines a polyhedron, and it is homeomorphic with a torus in case of a simple cube-curve. A curve in $\mathbb{R}^3$ is *complete* in $\mathbf{g}$ iff it has a nonempty intersection with every cube contained in g. Following [3, 4], we define:

Definition 1. *A* minimum-length polygon *(MLP) of a simple cube-curve g is a shortest simple curve P which is contained and complete in tube $\mathbf{g}$. The length of a simple cube-curve g is defined to be the length $l(P)$ of an* MLP *P of g.*

It turns out that such a shortest simple curve P is always a polygonal curve, and it is uniquely defined if the cube-curve is not only contained in a single layer of cubes of the 3D grid (see [3, 4]). If it is contained in one layer, then the MLP is uniquely defined up to a translation orthogonal to that layer. We speak about *the* MLP of a simple cube-curve.

A *critical edge* of a cube-curve g is such a grid edge which is incident with exactly three different cubes contained in g. Figure 1 shows all the critical edges of a simple cube-curve.

Definition 2. *If e is a critical edge of g and l is a straight line such that $e \subset l$, then l is called a* critical line of e in g *or* critical line *for short.*

Definition 3. *Let e be a critical edge of g. Let P_1 and P_2 be the two end points of e. If one of coordinates of P_1 is less than that of P_2, then P_1 is called the* first end point of e in g. *Otherwise P_1 is called the* second end point of e in g.

Definition 4. *Assume a simple cube-curve g and a triple of consecutive critical edges e_1, e_2, and e_3 such that $e_i \perp e_j$, for all $i, j = 1, 2, 3$ with $i \neq j$. If e_2 is parallel to the x-axis (y-axis, or z-axis) implies the x-coordinates (y-coordinates,* *or z-coordinates) of two vertices (i.e., end points) of* e_1 *and* e_3 *are equal, then we say that* e_1*,* e_2 *and* e_3 *form an* end angle*, and* g has an end angle*, denoted by* $\angle(e_1, e_2, e_3)$*; otherwise we say that* e_1*,* e_2 *and* e_3 *form a* middle angle*, and* g has a middle angle*.*

Figure 1 shows a simple cube-curve which has 5 end angles $\angle(e_{21}, e_0, e_1)$, $\angle(e_4, e_5, e_6)$, $\angle(e_6, e_7, e_8)$, $\angle(e_{14}, e_{15}, e_{16})$), $\angle(e_{16}, e_{17}, e_{18})$, and many middle angles (e.g., $\angle(e_0, e_1, e_2)$, $\angle(e_1, e_2, e_3)$, or $\angle(e_2, e_3, e_4)$).

Definition 5. *A simple cube-curve* g *is called* first class *iff each critical edge of* g *contains exactly one vertex of the MLP of* g*.*

We can simply detect a simple cube-curve is first class or not by running rubber band algorithm: the curve is first class iff option (O_1) (see [1]) does not occur.

This paper focuses on first-class simple cube-curves because the general simple cube-curves require further studies.

Definition 6. *Let* $S \subseteq \mathbb{R}^3$*. The set* $\{(x, y, 0) : \exists z(z \in \mathbb{R} \wedge (x, y, z) \in S)\}$ *is the* xy-projection *of* S*, or* projection *of* S *for short. Analogously we define the yz- or* xz-projection *of* S*.*

Definition 7. *If* e_1*,* e_2*, ...,* e_m *are consecutive critical edges of a cube-curve* g *and* $e_0 \perp e_1$*,* $e_m \perp e_{m+1}$*, and* $e_i \parallel e_{i+1}$*, where* i *equals 1, 2, ..., and* $m-1$*,* $m \geq 2$*, then* $\{e_1, e_2, \ldots, e_m\}$ *is a set of* maximal parallel critical edges *of* g*, and critical edge* e_0 *or* e_{m+1} *is called* adjacent to *this set.*

Figure 1 shows a simple cube-curve which has 2 maximal parallel critical edge sets: $\{e_{11}, e_{12}\}$ and $\{e_{18}, e_{19}, e_{20}, e_{21}\}$. The two adjacent critical edges of

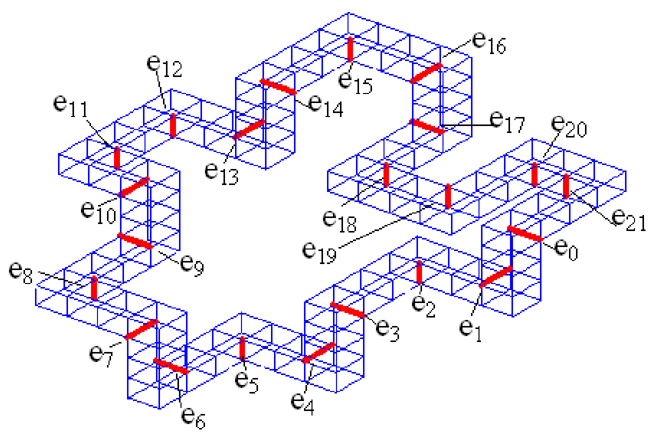

Fig. 1. Example of a first-class simple cube-curve which has middle and end angles

$\{e_{11}, e_{12}\}$ are e_{10} and e_{13}, they are on two different grid planes. The two adjacent critical edges of $\{e_{18}, e_{19}, e_{20}, e_{21}\}$ are e_{17} and e_0, they are on two different grid planes as well.

The paper is organized as follows: Section 2 describes theoretical fundamentals for constructing our example. Section 3 presents the example. Section 4 gives the conclusions.

2 Basics

We provide mathematical fundamentals used for constructing a simple cube-curve such that none of the vertices of its 3D MLP is a grid vertex. We start with citing a basic theorem from [1]:

Theorem 1. *Let g be a simple cube-curve. Critical edges are the only possible locations of vertices of the MLP of g.*

Let $d_e(p, q)$ be the Euclidean distance between points p and q.

Let e_0, e_1, e_2, ..., e_m and e_{m+1} be $m+2$ consecutive critical edges in a simple cube-curve, and let l_0, l_1, l_2, ..., l_m and l_{m+1} be the corresponding critical lines. We express a point $p_i(t_i) = (x_i + k_{x_i} t_i, y_i + k_{y_i} t_i, z_i + k_{z_i} t_i)$ on l_i in general form, with $t_i \in \mathbb{R}$, where i equals 0, 1, ..., or $m + 1$.

In the following, $p(t_i)$ will be denoted by p_i for short, where i equals 0, 1, ..., or $m + 1$.

Lemma 1. *If $e_1 \perp e_2$, then $\frac{\partial d_e(p_1,p_2)}{\partial t_2}$ can be written as $(t_2 - \alpha)\beta$, where $\beta > 0$, and β is a function of t_1 and t_2, α is 0 if e_1 and the first end point of e_2 are on the same grid plane, and α is 1 otherwise.*

Proof. Without loss of generality, we can assume that e_2 is parallel to z-axis. In this case, the parallel projection (denoted by $g'(e_1, e_2)$) of all of g's cubes, contained between e_1 and e_2, is illustrated in Figure 2, where AB is the projective image of e_1, and C is that of one of the end points of e_2.

Case 1. e_1 and the first end point of e_2 are on the same grid plane. Let the two end points of e_2 be (a, b, c) and $(a, b, c + 1)$. Then the two end points of e_1 are

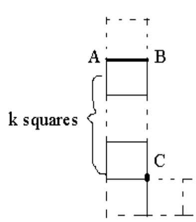

Fig. 2. Illustration of the proof of Lemma 1

$(a-1, b+k, c)$ and $(a, b+k, c)$. Then the coordinates of p_1 and p_2 are $(a-1+t_1, b+k, c)$ and $(a, b, c+t_2)$ respectively, and $d_e(p_1, p_2) = \sqrt{(t_1-1)^2 + k^2 + {t_2}^2}$.

Therefore $\frac{\partial d_e(p_1,p_2)}{\partial t_2} = \frac{t_2}{\sqrt{(t_1-1)^2+k^2+{t_2}^2}}$. Let $\alpha = 0$ and $\beta = \frac{1}{\sqrt{(t_1-1)^2+k^2+{t_2}^2}}$. This proves the lemma for Case 1.

Case 2. e_1 and the first end point of e_2 are on different grid planes (i.e., e_1 and the second end point of e_2 are on the same grid plane). Let the two end points of e_2 be (a, b, c) and $(a, b, c+1)$. Then the two end points of e_1 are $(a-1, b+k, c+1)$ and $(a, b+k, c+1)$. Then the coordinates of p_1 and p_2 are $(a-1+t_1, b+k, c+1)$ and $(a, b, c+t_2)$ respectively, and $d_e(p_1, p_2) = \sqrt{(t_1-1)^2 + k^2 + (t_2-1)^2}$.

Therefore $\frac{\partial d_e(p_1,p_2)}{\partial t_2} = \frac{t_2-1}{\sqrt{(t_1-1)^2+k^2+(t_2-1)^2}}$. Let $\alpha = 1$ and $\beta = \frac{1}{\sqrt{(t_1-1)^2+k^2+(t_2-1)^2}}$. This proves the lemma for Case 2. □

Lemma 2. *If* $e_1 \parallel e_2$, *then* $\frac{\partial d_e(p_1,p_2)}{\partial t_2}$ *can be written as* $(t_2 - t_1)\beta$, *where* $\beta > 0$, *and* β *is a function of* t_1 *and* t_2

Proof. Without loss of generality, we can assume that e_2 is parallel to z-axis. In this case, the parallel projection (denoted by $g'(e_1, e_2)$) of all of g's cubes contained between e_1 and e_2 is illustrated in Figure 3, where A is the projective image of one of the end points of e_1, and B is that of one of the end points of e_2.

Case 1. e_1 and e_2 are on the same grid plane. Let the two end points of e_2 be (a, b, c) and $(a, b, c+1)$. Then the two end points of e_1 are $(a, b+k, c)$ and $(a, b+k, c+1)$. Then the coordinates of p_1 and p_2 are $(a, b+k, c+t_1)$ and $(a, b, c+t_2)$ respectively, and $d_e(p_1, p_2) = \sqrt{(t_2-t_1)^2 + k^2}$.

Therefore $\frac{\partial d_e(p_1,p_2)}{\partial t_2} = \frac{t_2-t_1}{\sqrt{(t_2-t_1)^2+k^2}}$. Let $\beta = \frac{1}{\sqrt{(t_2-t_1)^2+k^2}}$. This proves the lemma for Case 1.

Case 2. e_1 and e_2 are on different grid planes. Let the two end points of e_2 be (a, b, c) and $(a, b, c+1)$. Then the two end points of e_1 are $(a-1, b+k, c)$ and

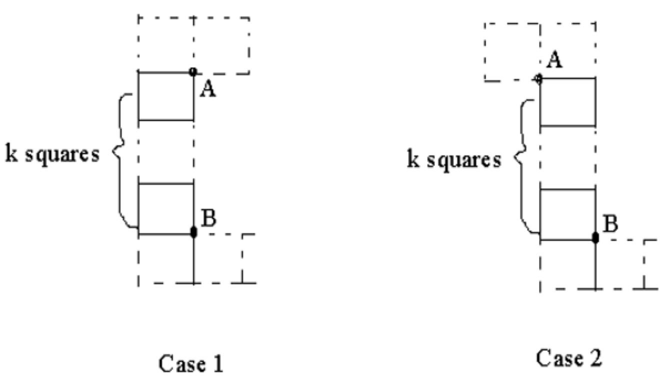

Fig. 3. Illustration of the proof of Lemma 2

$(a-1, b+k, c+1)$. Then the coordinates of p_1 and p_2 are $(a-1, b+k, c+t_1)$ and $(a, b, c+t_2)$ respectively, and $d_e(p_1, p_2) = \sqrt{(t_2-t_1)^2+k^2+1}$.

Therefore $\frac{\partial d_e(p_1,p_2)}{\partial t_2} = \frac{t_2-t_1}{\sqrt{(t_2-t_1)^2+k^2+1}}$. Let $\beta = \frac{1}{\sqrt{(t_2-t_1)^2+k^2+1}}$. This proves the lemma for Case 2. □

This Lemma will be used when we prove Lemma 6 later.

Let $d_i = d_e(p_{i-1}, p_i) + d_e(p_i, p_{i+1})$, where i equals 1, 2, ..., or m.

Theorem 2. *If $e_i \perp e_j$, where $i, j = 1, 2, 3$ and $i \neq j$, then e_1, e_2 and e_3 form an end angle iff the equation $\frac{\partial(d_e(p_1,p_2)+d_e(p_2,p_3))}{\partial t_2} = 0$ has a unique root 0 or 1.*

Proof. Without loss of generality, we can assume that e_2 is parallel to z-axis.

(A) If e_1, e_2 and e_3 form an end angle, then by Definition 4, the z-coordinates of two end points of e_1 and e_3 are equal.

Case A1. e_1, e_3 and the first end point of e_2 are on the same grid plane. By Lemma 1, $\frac{\partial(d_e(p_1,p_2))}{\partial t_2} = (t_2-\alpha_1)\beta_1$, where $\alpha_1 = 0$ and $\beta_1 > 0$, and $\frac{\partial(d_e(p_2,p_3))}{\partial t_2} = (t_2-\alpha_2)\beta_2$, where $\alpha_2 = 0$ and $\beta_2 > 0$. So we have $\frac{\partial(d_e(p_1,p_2)+d_e(p_2,p_3))}{\partial t_2} = t_2(\beta_1+\beta_2)$. Therefore the equation $\frac{\partial(d_e(p_1,p_2)+d_e(p_2,p_3))}{\partial t_2} = 0$ has a unique root $t_2 = 0$.

Case A2. e_1, e_3 and the second end point of e_2 are on the same grid plane. By Lemma 1, $\frac{\partial(d_e(p_1,p_2))}{\partial t_2} = (t_2-\alpha_1)\beta_1$, where $\alpha_1 = 1$ and $\beta_1 > 0$, and $\frac{\partial(d_e(p_2,p_3))}{\partial t_2} = (t_2-\alpha_2)\beta_2$, where $\alpha_2 = 1$ and $\beta_2 > 0$. So we have $\frac{\partial(d_e(p_1,p_2)+d_e(p_2,p_3))}{\partial t_2} = (t_2-1)(\beta_1+\beta_2)$. Therefore, equation $\frac{\partial(d_e(p_1,p_2)+d_e(p_2,p_3))}{\partial t_2} = 0$ has a unique root $t_2 = 1$.

(B) Conversely, if equation $\frac{\partial(d_e(p_1,p_2)+d_e(p_2,p_3))}{\partial t_2} = 0$ has a unique root 0 or 1, then e_1, e_2 and e_3 form an end angle. Otherwise, e_1, e_2 and e_3 form a middle angle. By Definition 4, the z-coordinates of two end points of e_1 are not equal to z-coordinates of two end points of e_3 (Note: Without loss of generality, we can assume that $e_2 \parallel z$-axis.). So e_1 and e_3 are not on the same grid plane.

Case B1. e_1 and the first end point of e_2 are on the same grid plane, while e_3 and the second end point of e_2 are on the same grid plane. By Lemma 1, $\frac{\partial(d_e(p_1,p_2))}{\partial t_2} = (t_2-\alpha_1)\beta_1$, where $\alpha_1 = 0$ and $\beta_1 > 0$, while $\frac{\partial(d_e(p_2,p_3))}{\partial t_2} = (t_2-\alpha_2)\beta_2$, where $\alpha_2 = 1$ and $\beta_2 > 0$. So we have $\frac{\partial(d_e(p_1,p_2)+d_e(p_2,p_3))}{\partial t_2} = t_2\beta_1 + (t_2-1)\beta_2$. Therefore $t_2 = 0$ or 1 is not a root of the equation $\frac{\partial(d_e(p_1,p_2)+d_e(p_2,p_3))}{\partial t_2} = 0$. This is a contradiction.

Case B2. e_1 and the second end point of e_2 are on the same grid plane, while e_3 and the first end point of e_2 are on the same grid plane. By Lemma 1, $\frac{\partial(d_e(p_1,p_2))}{\partial t_2} = (t_2-\alpha_1)\beta_1$, where $\alpha_1 = 1$ and $\beta_1 > 0$, while $\frac{\partial(d_e(p_2,p_3))}{\partial t_2} = (t_2-\alpha_2)\beta_2$, where $\alpha_2 = 0$ and $\beta_2 > 0$. So we have $\frac{\partial(d_e(p_1,p_2)+d_e(p_2,p_3))}{\partial t_2} = (t_2-1)\beta_1 + t_2\beta_2$. Therefore, $t_2 = 0$ or 1 is not a root of the equation $\frac{\partial(d_e(p_1,p_2)+d_e(p_2,p_3))}{\partial t_2} = 0$. This is a contradiction as well. □

Theorem 3. *If* $e_i \perp e_j$*, where* $i, j = 1, 2, 3$ *and* $i \neq j$*, then* e_1*,* e_2 *and* e_3 *form a middle angle iff the equation* $\frac{\partial(d_e(p_1,p_2)+d_e(p_2,p_3))}{\partial t_2} = 0$ *has a root* t_{2_0} *such that* $0 < t_{2_0} < 1$*.*

Proof. If e_1, e_2 and e_3 form a middle angle, then by Definition 4, e_1, e_2 and e_3 do not form an end angle. By Theorem 2, 0 or 1 is not a root of the equation $\frac{\partial(d_e(p_1,p_2)+d_e(p_2,p_3))}{\partial t_2} = 0$. By Lemma 1, $\frac{\partial(d_e(p_1,p_2)+d_e(p_2,p_3))}{\partial t_2} = (t_2 - \alpha_1)\beta_1 + (t_2 - \alpha_2)\beta_2$, where α_1, α_2 are 0 or 1, $\beta_1 > 0$ is a function of t_1 and t_2, and $\beta_2 > 0$ is a function of t_2 and t_3. So $\alpha_1 \neq \alpha_2$. (i.e., $\alpha_1 = 0$ and $\alpha_2 = 1$ or $\alpha_1 = 1$ and $\alpha_2 = 0$). Therefore the equation $\frac{\partial(d_e(p_1,p_2)+d_e(p_2,p_3))}{\partial t_2} = 0$ has a root t_{2_0} such that $0 < t_{2_0} < 1$.

Conversely, if the equation $\frac{\partial(d_e(p_1,p_2)+d_e(p_2,p_3))}{\partial t_2} = 0$ has a root t_{2_0} such that $0 < t_{2_0} < 1$, then by Theorem 2, e_1, e_2 and e_3 do not form an end angle. By Definition 4, e_1, e_2 and e_3 do form a middle angle. □

Assume that $e_0 \perp e_1$, $e_2 \perp e_3$, and $e_1 \parallel e_2$. Assume that $p(t_{i_0})$ is a vertex of the MLP of g, where i equals 1 or 2. Then we have

Lemma 3. *If* e_0*,* e_3 *and the first end point of* e_1 *are on the same grid plane, and* t_{i_0} *is a root of* $\frac{\partial d_i}{\partial t_i} = 0$*, then* $t_{i_0} = 0$*, where* i *equals 1 or 2.*

Proof. From $p_0(t_0)p_1(0) \perp e_1$ it follows that

$$d_e(p_0(t_0)p_1(0)) = \min\{d_e(p_0(t_0), p_1(t_1)) : t_1 \in [0, 1]\}$$

(see Figure 4). Analogously, we have $d_e(p_2(0)p_3(t_3)) = \min\{d_e(p_2(t_2), p_3(t_3)) : t_2 \in [0, 1]\}$ and $d_e(p_1(0)p_2(0)) = \min\{d_e(p_1(t_1), p_2(t_2)) : t_1, t_2 \in [0, 1]\}$. Therefore we have

$$\min\{d_e(p_0(t_0), p_1(t_1)) + d_e(p_1(t_1), p_2(t_2)) + d_e(p_2(t_2), p_3(t_3)) : t_1, t_2 \in [0, 1]\}$$
$$\geq d_e(p_0(t_0), p_1(0)) + d_e(p_1(0), p_2(0)) + d_e(p_2(0), p_3(t_3))$$ □

Assume that we have $e_0 \perp e_1$, $e_m \perp e_{m+1}$, and $e_i \parallel e_{i+1}$, (i.e., the set $\{e_1, e_2, \ldots, e_m\}$ is a set of maximal parallel critical edges of g, and e_0 or e_{m+1} is an adjacent critical edge of this set). Furthermore, let $p(t_{i_0})$ be a vertex of the MLP of g, where $i = 1, 2, \ldots, m-1$. Analogously, we have the following two lemmas:

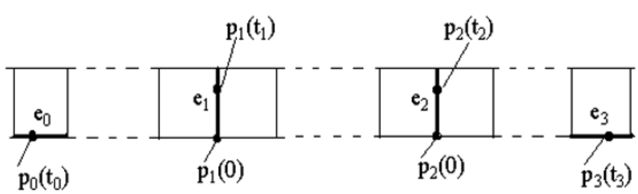

Fig. 4. Illustration of the proof of Lemma 3

Lemma 4. *If* e_0, e_{m+1} *and the first point of* e_1 *are on the same grid plane, and* t_{i_0} *is a root of* $\frac{\partial d_i}{\partial t_i} = 0$, *then* $t_{i_0} = 0$, *where* $i = 1, 2, \ldots, m$.

Lemma 5. *If* e_0, e_{m+1} *and the second end point of* e_1 *are on the same grid plane, and* t_{i_0} *is a root of* $\frac{\partial d_i}{\partial t_i} = 0$, *then* $t_{i_0} = 1$, *where* $i = 1, 2, \ldots, m$.

Lemma 6. *If* e_0 *and* e_{m+1} *are on different grid planes, and* t_{i_0} *is a root of* $\frac{\partial d_i}{\partial t_i} = 0$, *where* $i = 1, 2, \ldots, m$. *Then* $0 < t_1 < t_2 < \ldots < t_m < 1$.

Proof. Assume that e_0 and the first end point of e_1 are on the same grid plane, and e_{m+1} and the second end point of e_1 are on the same grid plane. Then by Lemmas 1 and 2, $\frac{\partial d_i}{\partial t_i}$, where $i = 1, 2, \ldots, m$, have the following forms: $\frac{\partial d_1}{\partial t_1} = t_1 b_{1_1} + (t_1 - t_2) b_{1_2}$, $\frac{\partial d_2}{\partial t_2} = (t_2 - t_1) b_{2_1} + (t_2 - t_3) b_{2_2}$, $\frac{\partial d_3}{\partial t_3} = (t_3 - t_2) b_{3_1} + (t_3 - t_4) b_{3_2}$, …, $\frac{\partial d_{m-1}}{\partial t_{m-1}} = (t_{m-1} - t_{m-2}) b_{m-1_1} + (t_{m-1} - t_m) b_{m-1_2}$, and $\frac{\partial d_m}{\partial t_m} = (t_m - t_{m-1}) b_{m_1} + (t_m - 1) b_{m_2}$, where $b_{i_1} > 0$, and b_{i_1} is a function of t_i and t_{i-1}, and $b_{i_2} > 0$, and b_{i_2} is a function of t_i and t_{i+1}, $i = 1, 2, \ldots, m$.

If $t_{1_0} < 0$, then by $\frac{\partial d_1}{\partial t_1} = 0$, we have $t_{1_0} b_{1_1} + (t_{1_0} - t_{2_0}) b_{1_2} = 0$. Since $b_{1_1} > 0$ and $b_{1_2} > 0$, so we have $t_{1_0} - t_{2_0} > 0$, (i.e., $t_{1_0} > t_{2_0}$). Analogously, by $\frac{\partial d_2}{\partial t_2} = 0$, so $(t_{2_0} - t_{1_0}) b_{2_1} + (t_{2_0} - t_{3_0}) b_{2_2} = 0$. Then we have $t_{2_0} > t_{3_0}$. Analogously, we have $t_{3_0} > t_{4_0}$, …, $t_{m-1_0} > t_{m_0}$. Therefore, by $\frac{\partial d_m}{\partial t_m} = (t_m - t_{m-1}) b_{m_1} + (t_m - 1) b_{m_2}$, we have $t_{m_0} - 1 > 0$. So we have $0 > t_{1_0} > t_{2_0} > t_{3_0} > \ldots > t_{m_0} > 1$. This is a contradiction.

If $t_{1_0} = 0$, then by $\frac{\partial d_1}{\partial t_1} = 0$ we have $t_{2_0} = 0$. Analogously, by $\frac{\partial d_2}{\partial t_2} = 0$ we have $t_{3_0} = 0$. Analogously, we have $t_{4_0} = 0$, …, $t_{m_0} = 0$. But, by $\frac{\partial d_m}{\partial t_m} = (t_m - t_{m-1}) b_{m_1} + (t_m - 1) b_{m_2}$, we have $\frac{\partial d_m}{\partial t_m} = (t_m - 1) b_{m_2} = -b_{m_2} < 0$. This is in contradiction to $\frac{\partial d_m}{\partial t_m} = 0$.

If $t_{1_0} \geq 1$, then by $\frac{\partial d_1}{\partial t_1} = 0$, we have $t_{1_0} b_{1_1} + (t_{1_0} - t_{2_0}) b_{1_2} = 0$. Due to $b_{1_1} > 0$ and $b_{1_2} > 0$ we have $t_{1_0} - t_{2_0} < 0$, (i.e., $t_{1_0} < t_{2_0}$). Analogously, by $\frac{\partial d_2}{\partial t_2} = 0$ it follows that $(t_{2_0} - t_{1_0}) b_{2_1} + (t_{2_0} - t_{3_0}) b_{2_2} = 0$. Then we have $t_{2_0} < t_{3_0}$. Analogously, we have $t_{3_0} < t_{4_0}$, …, $t_{m-1_0} < t_{m_0}$. Therefore, by $\frac{\partial d_m}{\partial t_m} = (t_m - t_{m-1}) b_{m_1} + (t_m - 1) b_{m_2}$, we have $t_{m_0} - 1 < 0$. So we have $1 \leq t_{1_0} < t_{2_0} < t_{3_0} < \ldots < t_{m_0} < 1$. This is a contradiction. □

Let t_{i_0} be a root of $\frac{\partial d_i}{\partial t_i} = 0$, where $i = 1, 2, \ldots, m$. We apply Lemmas 4, 5 and 6 and obtain

Theorem 4. e_0 *and* e_{m+1} *are on different grid plane iff* $0 < t_{1_0} < t_{2_0} < \ldots < t_{m_0} < 1$.

3 An Example

We provide one example to show that there is a simple cube-curve such that none of the vertices of its 3D MLP is a grid vertex. See Table 1, which lists the coordinates of the critical edges $e_0, e_1, \ldots, e_{19}$ of g. Let $v(t_0), v(t_1), \ldots, v(t_{19})$ be

Table 1. Coordinates of endpoints of critical edges in Figure 5

Critical edge	x_{i1}	y_{i1}	z_{i1}	x_{i2}	y_{i2}	z_{i2}
e_0	-1	4	7	-1	4	8
e_1	1	4	7	1	5	7
e_2	2	4	5	2	5	5
e_3	4	5	4	4	5	5
e_4	4	7	4	5	7	4
e_5	5	7	2	5	8	2
e_6	7	7	2	7	8	2
e_7	7	8	4	8	8	4
e_8	8	10	4	8	10	5
e_9	10	10	4	10	10	5
e_{10}	10	8	5	11	8	5
e_{11}	11	7	7	11	8	7
e_{12}	12	7	7	12	7	8
e_{13}	12	5	7	12	5	8
e_{14}	10	4	8	10	5	8
e_{15}	9	4	10	10	4	10
e_{16}	9	0	10	10	0	10
e_{17}	9	0	8	10	0	8
e_{18}	9	1	7	9	1	8
e_{19}	-1	2	7	-1	2	8

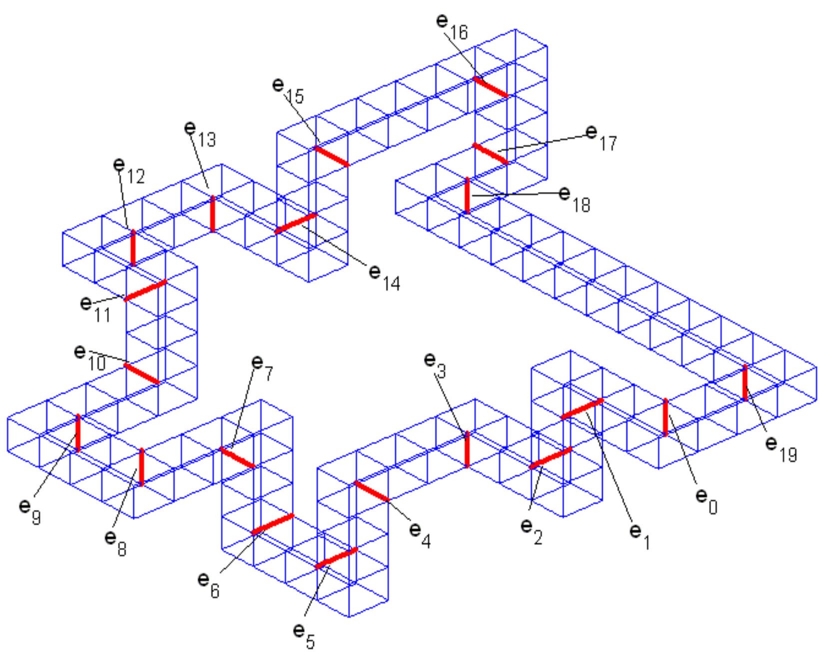

Fig. 5. A simple cube-curve such that none of the vertices of its 3D MLP is a grid vertex

the vertex of the MLP of g such that $v(t_i)$ is on e_i and t_i is in [0, 1], where i = 0, 1, 2, ..., 19. By Appendix we can see that there is not any end angle in g. In fact, there are 6 middle angles: $\angle(e_2, e_3, e_4))$, $\angle(e_3, e_4, e_5))$, $\angle(e_6, e_7, e_8))$, $\angle(e_9, e_{10}, e_{11}))$, $\angle(e_{10}, e_{11}, e_{12}))$, and $\angle(e_{13}, e_{14}, e_{15}))$. By Theorem 3, we have $t_3, t_4, t_7, t_{10}, t_{11}$ and t_{14} are in (0, 1). By Figure 5 we can see that $e_1 \parallel e_2$ and e_0 and e_3 are on different grid planes. By Theorem 4, we have t_1 and t_2 are in (0, 1).

Analogously, we have t_5 and t_6 are in (0, 1); t_8 and t_9 are in (0, 1); t_{12} and t_{13} are in (0, 1); t_{15}, t_{16} and t_{17} are in (0, 1); and t_{18}, t_{19} and t_0 are in (0, 1). Therefore, each t_i is in (0, 1), where $i = 0, 1, \ldots, 19$. So g is a simple cube-curve such that none of the vertices of its 3D MLP is a grid vertex.

4 Conclusions

We have constructed a non-trivial simple cube-curve such that none of the vertices of its 3D MLP is a grid vertex. Indeed, by Theorems 2 and 4, and Lemmas 5 and 6, we can come to the conclusion that given a simple first class cube-curve g, none of the vertices of its 3D MLP is a grid point iff g has not any end angle and for every set of maximal parallel edges of g, its two adjacent critical edges are not on the same grid plane.

It follows that the (provable correct) MLP algorithm proposed in [6] cannot be applied to this curve, because it requires at least one end angle for decomposing the curve into arcs. Of course, the rubber-band algorithm is applicable, and will produce a result (i.e., a polygonal curve). However, in this case we are still unable to show whether this result is the MLP of the given cube-curve or not.

Acknowledgements. The reviewers' comments have been very helpful for revising an earlier version of this paper.

Appendix: List of $\frac{\partial d_i}{\partial t_i}$ (i = 0, 1, ..., 19)

We compute $\frac{\partial d_i}{\partial t_i}$ (i = 0, 1, ..., 19) for g as shown in Figure 5.

$$d_{t_0} = \frac{t_0}{\sqrt{{t_0}^2 + {t_1}^2 + 4}} + \frac{t_0 - t_{19}}{\sqrt{(t_0 - t_{19})^2 + 4}} \tag{1}$$

$$d_{t_1} = \frac{t_1}{\sqrt{{t_0}^2 + {t_1}^2 + 4}} + \frac{t_1 - t_2}{\sqrt{(t_1 - t_2)^2 + 5}} \tag{2}$$

$$d_{t_2} = \frac{t_2 - t_1}{\sqrt{(t_2 - t_1)^2 + 5}} + \frac{t_2 - 1}{\sqrt{(t_2 - 1)^2 + (t_3 - 1)^2 + 4}} \tag{3}$$

$$d_{t_3} = \frac{t_3 - 1}{\sqrt{(t_2 - 1)^2 + (t_3 - 1)^2 + 4}} + \frac{t_3}{\sqrt{{t_3}^2 + {t_4}^2 + 4}} \tag{4}$$

$$d_{t_4} = \frac{t_4}{\sqrt{{t_3}^2 + {t_4}^2 + 4}} + \frac{t_4 - 1}{\sqrt{(t_4 - 1)^2 + {t_5}^2 + 4}} \tag{5}$$

$$d_{t_5} = \frac{t_5}{\sqrt{(t_4-1)^2+{t_5}^2+4}} + \frac{t_5-t_6}{\sqrt{(t_5-t_6)^2+4}} \tag{6}$$

$$d_{t_6} = \frac{t_6-t_5}{\sqrt{(t_6-t_5)^2+4}} + \frac{t_6-1}{\sqrt{(t_6-1)^2+{t_7}^2+4}} \tag{7}$$

$$d_{t_7} = \frac{t_7}{\sqrt{(t_6-1)^2+{t_7}^2+4}} + \frac{t_7-1}{\sqrt{(t_7-1)^2+{t_8}^2+4}} \tag{8}$$

$$d_{t_8} = \frac{t_8}{\sqrt{(t_7-1)^2+{t_8}^2+4}} + \frac{t_8-t_9}{\sqrt{(t_8-t_9)^2+4}} \tag{9}$$

$$d_{t_9} = \frac{t_9-t_8}{\sqrt{(t_9-t_8)^2+4}} + \frac{t_9-1}{\sqrt{(t_9-1)^2+{t_{10}}^2+4}} \tag{10}$$

$$d_{t_{10}} = \frac{t_{10}}{\sqrt{(t_9-1)^2+{t_{10}}^2+4}} + \frac{t_{10}-1}{\sqrt{(t_{10}-1)^2+(t_{11}-1)^2+4}} \tag{11}$$

$$d_{t_{11}} = \frac{t_{11}-1}{\sqrt{(t_{11}-1)^2+(t_{10}-1)^2+4}} + \frac{t_{11}}{\sqrt{{t_{11}}^2+{t_{12}}^2+1}} \tag{12}$$

$$d_{t_{12}} = \frac{t_{12}}{\sqrt{{t_{11}}^2+{t_{12}}^2+1}} + \frac{t_{12}-t_{13}}{\sqrt{(t_{12}-t_{13})^2+4}} \tag{13}$$

$$d_{t_{13}} = \frac{t_{13}-t_{12}}{\sqrt{(t_{13}-t_{12})^2+4}} + \frac{t_{13}-1}{\sqrt{(t_{13}-1)^2+(t_{14}-1)^2+4}} \tag{14}$$

$$d_{t_{14}} = \frac{t_{14}-1}{\sqrt{(t_{13}-1)^2+(t_{14}-1)^2+4}} + \frac{t_{14}}{\sqrt{{t_{14}}^2+(t_{15}-1)^2+4}} \tag{15}$$

$$d_{t_{15}} = \frac{t_{15}-1}{\sqrt{{t_{14}}^2+(t_{15}-1)^2+4}} + \frac{t_{15}-t_{16}}{\sqrt{(t_{15}-t_{16})^2+16}} \tag{16}$$

$$d_{t_{16}} = \frac{t_{16}-t_{15}}{\sqrt{(t_{16}-t_{15})^2+16}} + \frac{t_{16}-t_{17}}{\sqrt{(t_{16}-t_{17})^2+4}} \tag{17}$$

$$d_{t_{17}} = \frac{t_{17}-t_{16}}{\sqrt{(t_{17}-t_{16})^2+4}} + \frac{t_{17}}{\sqrt{{t_{17}}^2+(t_{18}-1)^2+1}} \tag{18}$$

$$d_{t_{18}} = \frac{t_{18}-1}{\sqrt{{t_{17}}^2+(t_{18}-1)^2+1}} + \frac{t_{18}-t_{19}}{\sqrt{(t_{18}-t_{19})^2+101}} \tag{19}$$

$$d_{t_{19}} = \frac{t_{19}-t_{18}}{\sqrt{(t_{19}-t_{18})^2+101}} + \frac{t_{19}-t_0}{\sqrt{(t_{19}-t_0)^2+4}} \tag{20}$$

References

1. T. Bülow and R. Klette. Digital curves in 3D space and a linear-time length estimation algorithm. *IEEE Trans. Pattern Analysis Machine Intelligence*, **24**:962–970, 2002.
2. R. Klette and A. Rosenfeld. Digital Geometry: Geometric Methods for Digital Picture Analysis. Morgan Kaufmann, San Francisco, 2004., 2004.
3. F. Sloboda, B. Zaťko, and R. Klette. On the topology of grid continua. SPIE *Vision Geometry VII,* **3454**:52–63, 1998.
4. F. Sloboda, B. Zaťko, and J. Stoer. On approximation of planar one-dimensional grid continua. In R. Klette, A. Rosenfeld, and F. Sloboda, editors, *Advances in Digital and Computational Geometry*, pages 113–160. Springer, Singapore, 1998.
5. A. Jonas and N. Kiryati. Length estimation in 3-D using cube quantization, *J. Math. Imaging and Vision*, **8**: 215–238, 1998.
6. F. Li and R. Klette. Minimum-length polygon of a simple cube-curve in 3D space. In Proceedings IWCIA2004, LNCS3322 (to appear).
7. J. Canny and J.H. Reif. New lower bound techniques for robot motion planning problems. Proc. *IEEE Conf. Foundations Computer Science*, pages 49–60, 1987.
8. J. Choi, J. Sellen, and C.-K. Yap. Approximate Euclidean shortest path in 3-space. Proc. *ACM Conf. Computational Geometry*, ACM Press, pages 41–48, 1994.